Proceedings of the XVIII ECSMGE 2024
GEOTECHNICAL ENGINEERING CHALLENGES
TO MEET CURRENT AND EMERGING NEEDS OF SOCIETY

ISBN 978-1-032-54816-6
DOI 10.1201/9781003431749-510

ECSMGE 24
XVIII EUROPEAN CONFERENCE ON SOIL MECHANICS AND GEOTECHNICAL ENGINEERING

Large-scale test on basal steel-reinforced piled embankments

Essai à grande échelle sur les remblais basaux en pieux renforcés par de l'acier

M. Schneider*
Technical University of Darmstadt, Institute of Geotechnics, Germany

M. Hell, P. Pandrea
Keller Holding, Germany

B. Wittekoek, S.J.M. van Eekelen
Deltares, Netherlands

M. Topolnicki
Keller Polska, Poland

K. Makowska, R. Sieńko
SHM System, Poland

H. Zachert
Technical University of Darmstadt, Institute of Geotechnics, Germany

**marc.schneider1@tu-darmstadt.de*

ABSTRACT: This paper presents a novel large-scale test setup at TU Darmstadt to investigate the behaviour of basal reinforced piled embankments. The study focuses on the impact of welded steel mesh reinforcement. The study addresses key questions related to soil arching, deformations, strain distribution in the embankment and the steel mesh grid. The large-scale test setup, 25 m^2, at a 1:1.6 scale, includes 16 piles, a dry medium coarse river sand fill, a steel mesh reinforcement and a two-step system to model the soft soil compaction. State-of-the-art Distributed Fibre Optic Sensing (DFOS) technology enabled precise monitoring of soil and reinforcement strain and 3D deformation. Results indicate that the reinforcement stiffness minimally affects soil arching, matching the Concentric Arches (CA) model (van Eekelen et al., 2013, 2015) that was developed for geosynthetic reinforced piled embankments (GRPS). The deformation pattern and strain distribution in the steel differ from GRPS, illustrating the need for a specific load-deflection model. The measured critical height matches the prediction of Topolnicki and Kłosiński et al. (2022). The study contributes to understanding the complex interaction between steel reinforcement and soft soil in piled embankments, guiding future design considerations.

RÉSUMÉ: Cet article présente un nouveau dispositif d'essai à grande échelle à l'Université Technique de Darmstadt pour étudier le comportement des remblais sur pieux renforcés par une nappe de treillis soudés. L'étude se concentre sur l'impact de l'armature en treillis soudé sur les mécanismes de transferts de charge. L'étude aborde des questions clés liées à l'effet d'arche du sol, aux tassements et à la distribution des déformations dans le remblai et dans le treillis soudé. L'installation d'essai à grande échelle, 25 m^2, à l'échelle 1:1,6, comprend 16 pieux, un remblai de sable fluviatile moyennement grossier sec, un renforcement en treillis soudé et un système double pour modéliser le tassement du sol meuble. La technologie de pointe de la détection par fibre optique répartie (DFOS) a permis un contrôle précis du tassement du sol et du treillis soudé ainsi qu'une visualisation de la déformation en 3D. Les résultats indiquent que la rigidité du renforcement affecte peu la formation d'arches dans le sol, ce qui correspond au modèle d'arches concentriques (van Eekelen et al., 2013, 2015) qui a été développé pour les remblais sur pieux renforcés par des géosynthétiques (GRPS). La déformation et la distribution des contraintes dans l'acier sont différentes de ceux du GRPS, illustrant la nécessité d'un modèle charge-déformation spécifique. La hauteur critique de remblai mesurée correspond à la prédiction de Topolnicki et Kłosiński et al. (2022). L'étude contribue à la compréhension de l'interaction complexe entre le treillis soudé et le sol mou dans les remblais sur pieux, guidant les considérations de dimensionnement futurs.

Keywords: Piled embankments; steel basal reinforcement; large-scale physical modelling; distributed fibre optic sensing.

1 INTRODUCTION

Reinforced piled embankments with a geosynthetic reinforcement (GR) are commonly built in soft soil areas (van Eekelen and Han, 2020). Replacing GR for steel reinforcement (SR) is particularly appealing to reduce deformations caused by high embankments (Topolnicki et al., 2019).

This paper presents a large-scale test setup, nearly in full scale, 1:1.6, constructed at TU Darmstadt to allow investigation of piled embankments with basal reinforcement made of steel or geosynthetics. The test setup is part of a broader research initiative called PEBSTER (Piled Embankments with Basal Steel Reinforcement), including small-scale tests (van Eekelen et al., 2024) to investigate the following:

1. Does the soil arching in a piled embankment differ if SR is used instead of GR?
2. Are deformations different with SR instead of GR?
3. What is the influence of flexible vs. rigid piles?
4. Do the answers to these questions depend on the scale of model tests?
5. Can the current design methods for piled embankments using GR be applied for SR or do they require a modification?

2 LOAD DISTRIBUTION

Soil arching develops when soil between piles deforms more than the piles, resulting in a non-uniform load distribution. A significant portion of the vertical load (labelled as 'A' in Figure 1) is directly transferred to the piles. The residual load, 'B+C' in Figure 1, is supported by the subsurface between the piles.

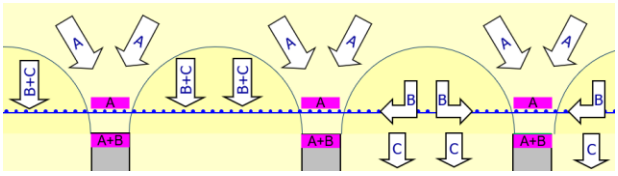

Figure 1. Load distribution in a PS embankment.

Several design guidelines and standards, such as BS8006 (2010), EBGEO (2011), ASIRI (2013), CUR226 (2016), and Topolnicki and Kłosiński et al. (2022), provide equations to divide the total vertical load into A and B+C. These guidelines then offer methods for calculating the strain in the reinforcement from the acting load B+C, considering the load-deflection behaviour of the reinforcement.

Many researchers have investigated the influence of geometry and material properties on soil arching. Van Eekelen et al. (2012) showed that the soil arching quickly develops, even when the deflection of the GR is minimal. In line with this finding, they showed that the GR tensile stiffness has a limited impact on soil arching, while the shear properties of the fill (internal friction angle) play a significant role. These conclusions were valid for GR. An important question of the PESBTER project is, whether the high axial and bending stiffness of the SR affects the soil arching in the fill.

3 LARGE-SCALE TEST SETUP

Figure 2 depicts the test setup designed to model piled embankments with a steel basal reinforcement. The model embankment represents a prototype embankment of 4.7 m height above the pile head.

This test setup was constructed within a part of the geotechnical test pit at the Institute of Geotechnics of TU Darmstadt. It occupies a base area of 5 by 5 m and has a total height of 5.5 m. The test setup includes 16 piles passing through the layer of soft soil model.
The embankment fill was modelled using dry medium coarse river sand ('Darmstadt Sand'). The soil model was installed by means of air pluviation achieving a mean density of 1.735 g/cm³, equivalent to 92 % relative density, and $\varphi'_{cv} = 34.8^{o}$.

The choice of a model embankment height of H = 2.9 m was determined by geometric scaling, in line with typical dimensions found in real piled embankments. This decision also took into consideration to safely surpass the critical height estimate of 1.52 m according to Topolnicki and Kłosiński et al. (2022), where the critical height represents the minimum vertical distance above the pile heads to reach a plane of uniform settlement above and between the supports. Concentrating soil pressure, strain and deformation measurements in the range between piles and critical height allows a thorough analysis of soil arching behaviour in the embankment.

3.1 Piles

The 16 piles are modelled using hollow S235 steel tubes with an outer diameters d = 244.5 mm and a wall thickness of t = 6.3 mm.

To better recreate the surface roughness found in concrete piles, the very smooth surface of the steel tubes was altered. The pile skin in contact with the sand layer above the soft soil model was covered with epoxy resin and poured sand. The pile skin below was not modified but kept smooth.

Previous experiments usually neglected pile settlements by using rigid supports. Natural load-bearing layers are stiff, but usually not rigid. To investigate the effect of flexible supports on the soil arching and load distribution behaviour the pile bases were equipped with springs with a stiffness of 5 MN/m (Figure 2). The LVDT transducer in the centre measures pile settlement and allows to derive the pile base force using spring calibration.

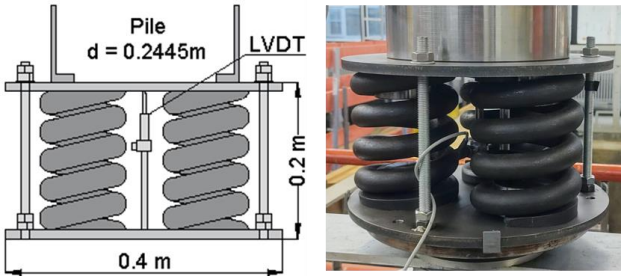

Figure 2. Three springs below each pile base, modelling a system with flexible supports.

Vertical loads acting on pile heads and pile settlements at the pile base were measured on 10 out of 16 piles to capture the behaviour of centre, edge and corner piles (Figure 2). Specially constructed pile heads, accommodating a standard load cell, allowed to measure the resulting vertical pile load directly.

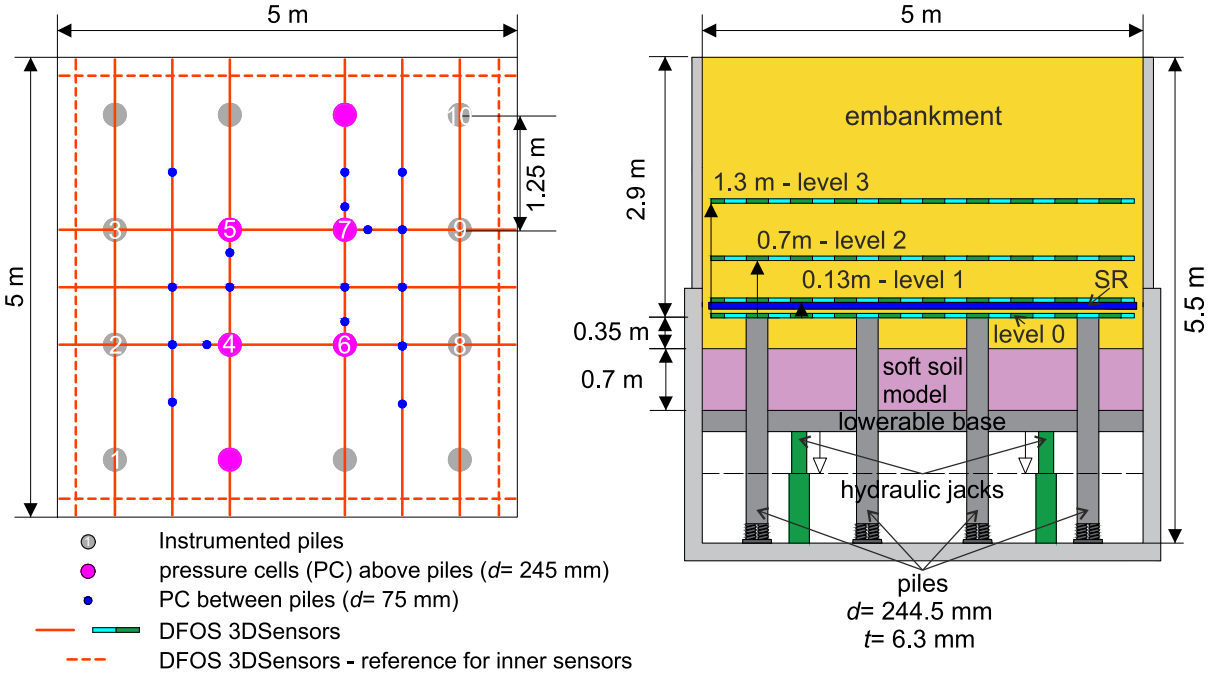

Figure 3. Large-scale test setup for basal reinforced piled embankments.

3.2 Soft soil model

The soft soil below the embankment was modelled using crumb rubber with grains of 1.5 to 5 mm in diameter. The rubber layer thickness was 0.7 m, with an average density of 0.48 g/cm³. To investigate the one-dimensional compressibility of the rubber, a special oedometer test was carried out using a specimen 285 mm in diameter and 50 mm in height and with a comparable initial density. The data presented in Figure 4 illustrate that crumb rubber tends to creep after each loading step.

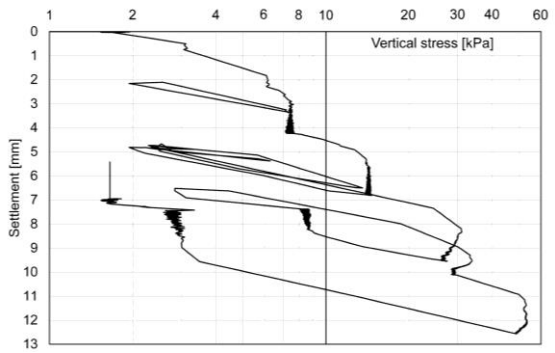

Figure 4. Large oedometer test of crumb rubber.

Also, after unloading steps there is a noticeable rebound of deformation under a stable load. Further analyses of the crumb rubber behaviour will therefore be required.

Due to consolidation and creep of soft soils, the subsoil reaction C can disappear over time. To model this situation, the rubber layer was placed on a stiff base supported by four hydraulic jacks. At the end of the test, the base plate was lowered incrementally 220 mm in total, creating a partial void below the steel mesh.

3.3 Steel mesh reinforcement

The basal steel mesh reinforcement consists of 8 mm ribbed bars (S235 steel), welded with a c/c spacing of 100×100 mm. The resulting tensile and bending stiffnesses of the mesh are EA = 105558 kN/m and EI = 0.2577 kN·m²/m, respectively.

In practice, steel meshes are produced in sheets and are connected on site using overlapping across and steel hooks along the embankment. The model arrangement consists of three sheets S1 to S3 (Figure 5). Sheet S1, with a size of 2.5×5 m, is connected with hooks to two smaller meshes S2 and S3, while S2 and S3 are connected by overlapping. In total, 49 hooks were used, and 16 of them were equipped with strain gauges to measure strain and study the interactions between the separate sheets.

3.4 Instrumentation

The development of soil arching begins near the pile heads when the soil in between piles starts to settle more than the piles themselves. To study this, the majority of the sensors were placed close to the pile heads and above or surrounding the piles. In total, 52 carefully selected sensors were used to measure forces, pressures and displacements in the system to allow an insight into the load distribution pattern as well as total loads at the system boundaries. Table 1 lists the mentioned sensors.

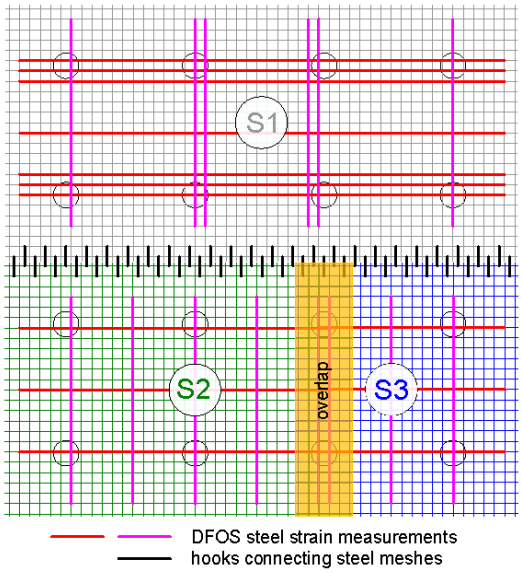

Figure 5. The arrangement of steel sheets S1, S2 and S3 in the test setup, and the location of the overlap and hooks.

Table 1. Measurement equipment for loads, pressures and vertical displacements.

Sensor Type	Quantity	Location [level]
Force	10	Pile head [0]
Pressure	6	Above pile locations [1]
Pressure	18	Distributed on SR between piles [0, 1]
Total load	4	Below model base frame
Displacement	10	Pile base
Displacement	4	Model base frame

Table 2. Measurement equipment for soil and reinforcement strains and displacements.

Sensor Type	Quantity	Location [level]
Strain in steel bars	8	DFOS steel strain, glued to the bars [1]
DFOS EpsilonSensor	2	DFOS soil strain [1]
DFOS 3DSensor	40	All levels [0-4]
Reference displ. DFOS	16	Outer test setup walls

Table 2 gives an overview of the sensors used to capture strains and deformation in the system, either by conventional strain gauges or by distributed fibre optical sensors (DFOS) from the Nerve-Sensor family.

In total, 40 DFOS 3DSensors were used to capture soil and steel deformation at four different levels (Figure 2). Each 3DSensor consists of four strain fibres that measure strains along the sensors' length and allow calculation of deformations in three directions. However, the results shown in this paper solely consider vertical displacements due to the mainly vertical nature of deformation of the system.

The 3DSensors were installed in a grid to measure deformations and strains above and between the piles. Figure 2 (left) shows the DFOS grid at level 1. The DFOS sensors at level 2 were identical, while levels 0 and 3 had a reduced number of sensors.

Furthermore, eight optic fibres were glued to the steel mesh to capture steel strains, and two DFOS EpsilonSensors were installed to measure soil strains.

The level 1 DFOS 3DSensors were placed directly on the SR, effectively measuring the deflection of the steel bars. Levels 2 and 3 were located at chosen elevations to study soil deformations inside the embankment in the middle and close to the upper boundary of the expected soil arching.

4 RESULTS

4.1 Load distribution

Figure 6 compares the measured load part that was transferred to the piles via soil arching (load part A) during embankment construction with values calculated using established analytical models, developed for geosynthetic reinforcement. They do not consider reinforcement bending stiffness as an input parameter. Nevertheless, the measured values match the calculations reasonably well.

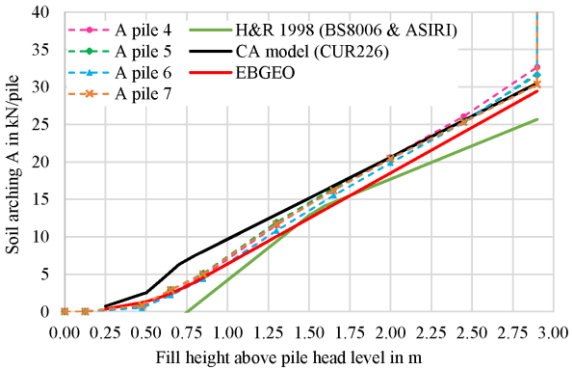

Figure 6. Load part A measured in the test and calculated with analytical models during embankment construction.

This analysis together with the findings of van Eekelen et al., 2024 supports the statement that the reinforcement stiffness does not have a significant impact on the load distribution pattern in the system (arching). Since the test only displays one combination of reinforcement stiffness and soil friction angle, further investigations are needed to experimentally confirm this conclusion.

4.2 Observed deformation pattern

Figure 7 a shows the measured vertical deformations at level 1, just above the steel. The graph includes two perpendicular directions over the whole model width, at the moment the full embankment height had just been achieved (test stage T2). In all unit cells, the deformation pattern is rather similar, validating the expected model performance and confirming the high quality of the applied monitoring system. Each of the following plots in Figure 7 shows data solely for the unit cell comprising the four inner piles.

Figures 7 b and 7 d show the absolute vertical deformation of the steel mesh at level 1 and levels 2 and 3, respectively, observed during three stages of the test, including the lowering of the model base frame (T3). To facilitate a direct and consistent comparison of these measurements, obtained at different locations and levels, the data have been normalized with respect to 'base lines'. These base lines connect the peaks in the deformed steel grid, above the (relatively rigid) piles. The measured deformations were normalised with respect to these base lines, and the normalised results are plotted in Figures 7 c and 7 e. They illustrate a more or less symmetrical deformation pattern at all levels and increasing deformation during successive stages of the test. Soil arching is caused by the differential deformation of the steel mesh above and between piles (Figure 7 c). Differential deflections of the steel bars running through the centre between the piles start to develop already during early embankment construction with average field centre deflections of 15.6 mm for 1.05 m high embankment. With progressing embankment height and the subsequent reduction of subsoil support, the differential deflections increase significantly, up to 32.4 mm in-between piles.

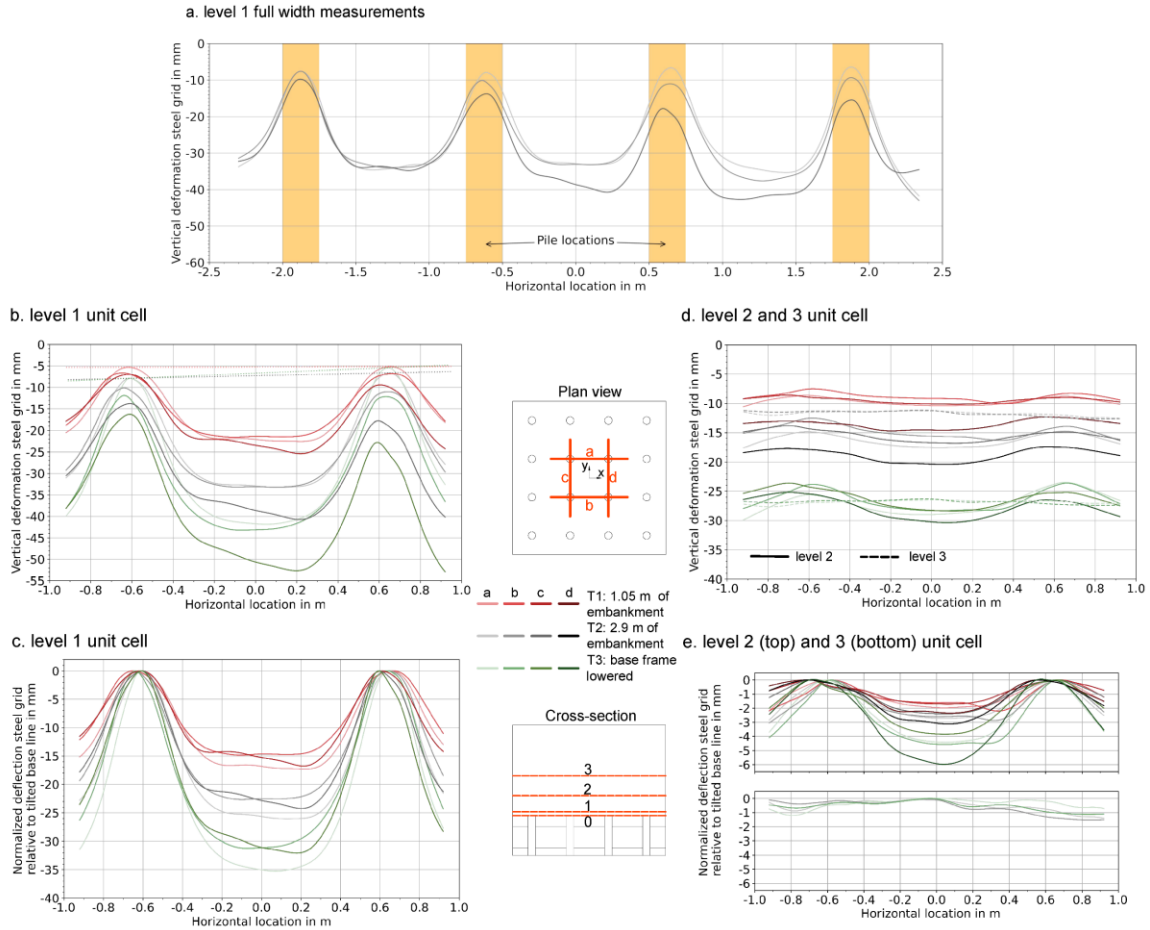

Figure 7. Measured vertical displacements of the steel mesh during and after embankment construction and after the removal of the subsoil support. a. full width, unaltered measurements above piles at stage T2. B. and d. Measured deflections of levels 1, 2 and 3 at stages T1, T2 and T3, along lines a, b, c, d and tilted base lines (b for level 1, and d for levels 2 and 3). c. and e. as b and d, but presented relative to the tilted base lines.

When comparing deformations in levels 2 and 3 (Figures 7 d and 7 e), a significant decrease of absolute and differential settlement is visible, indicating that the plane of equal settlement (critical embankment height) is located slightly above level 3, which is in line with the prediction of Topolnicki and Kłosiński et al. (2022).

5 CONCLUSIONS

This paper presents a large-scale model test on steel-reinforced piled embankments. This is part of a larger research, that also includes a series of small-scale tests and numerical analyses. Based on the test results presented in this paper, we draw the following preliminary conclusions.

- The reinforcement tensile and bending stiffness do not significantly affect the soil arching. This is supported by the test data of the stiff SR matching analytical calculations for load A for GR and the observations made by van Eekelen et al. (2024).
- Three main European design methods for GRPS embankments closely align with the measured soil arching, with the CA model exhibiting the best match.
- The high spatial resolution of DFOS sensors allows a unique look into the soil model and a thorough comparison of measured deformations and strains with calculated values.
- The steel reinforcement shows significant differential deflection and steel strain in the bars that bridge adjacent piles. This is in line with the deformation pattern observed in geosynthetic-reinforced piled embankments.
- The strain distributions in steel reinforcement differ from geosynthetic reinforcement. The main calculation models for geosynthetics assume zero reinforcement strain above the piles, assuming that the geosynthetic is clamped between soil and pile cap. The steel reinforcement in this test shows strains both in between and above the piles.

ACKNOWLEDGEMENTS

The authors are grateful for the funding received from the European Union's Horizon 2020 research and innovation program under Grant Agreement No. 101006512 for the transnational GEOLAB project PEBSTER, the TKI-PPS funding of the Dutch Ministry of Economic Affairs and the financial and practical support of Keller.

REFERENCES

ASIRI (2013). Recommendations for the design, construction and control of rigid inclusions ground improvements (French version is of 2012).

BS8006-1 (2010). Code of practice for strengthened/reinforced soils and other fills. British Standards Institution, UK.

CUR226 (2016). See Van Eekelen & Brugman (2016).

EBGEO (2011). Recommendations for Design and Analysis for Earth Structures using Geosynthetic Reinforcements (German version is of 2010).

Hewlett, W.J. and Randolph, M.F. (1988). Analysis of piled embankments. Ground Engineering, 21(3): 12-18.

Topolnicki, M., Sołtys, G., Brzozowski, T., 2019. Performance and modelling of road embankment supported on rigid inclusions and a transfer platform with steel geogrid, Proc. of the XVII ECSMGE-2019, Geotechnical Engineering foundation of the future, Reykjavik. DOI: 10.32075/17ECSMGE-2019-0811.

Topolnicki, M., Kłosiński, B. (eds.) et al., 2022. Recommendations for Ground Improvement with Rigid Inclusions - Design, Execution and Control (in Polish). PWN SA. ISBN 978-83-01-22578-0.

van Eekelen, S.J.M., Nancey, A., Bezuijen, A. (2012). Influence of fill material and type of geosynthetic reinforcement in a piled embankment, model experiments. In: Proc. Eur. Geosynthetic Congress., Valencia, Spain, Vol 5, 167-171.

van Eekelen, S.J.M., Bezuijen, A. van Tol, A.F., (2013). An analytical model for arching in piled embankments. Geotextiles and Geomembranes 39: 78-102. DOI: https://doi.org/10.1016/j.geotexmem.2013.07.005.

Van Eekelen, S.J.M., Bezuijen, A., van Tol, A.F., (2015). Validation of analytical models for the design of basal reinforced piled embankments. Geotextiles and Geomembranes Volume 43, Issue 1, 56 – 81. DOI: https://doi.org/10.1016/j.geotexmem.2014.10.002.

van Eekelen, S.J.M. & Brugman, M.H.A., Eds. (2016). Design Guideline Basal Reinforced Piled Embankments (CUR226). CRC press, Delft, Netherlands.

van Eekelen, S.J.M. and Han, J. (2020). Geosynthetic-reinforced pile-supported embankments: state of the art. Geosynthetics International 27 (2) 112-141. DOI: https://doi.org/10.1680/jgein.20.00005.

van Eekelen, S.J.M, Schneider, M., Hell, M., Wittekoek, B., Makowska, K., Zdanowicz, K., Pandrea, P., Sieńko, R., Schauber, P., Topolnicki, M., Zachert, H., (2024). 3D small-scale tests on steel-reinforced piled embankments. In: Proc. ECSMGE 24, Lisbon, Portugal.